Histone deacetylase inhibitor-induced cell death in bladder cancer is associated with chromatin modification and modifying protein expression: A proteomic approach

QINGDI QUENTIN LI[1], JIAN-JIANG HAO[2], ZHENG ZHANG[2], IAWEN HSU[1], YI LIU[2], ZHEN TAO[2], KEIDREN LEWI[1], ADAM R. METWALLI[1] and PIYUSH K. AGARWAL[1]

[1]Urologic Oncology Branch, Center for Cancer Research, National Cancer Institute, National Institutes of Health, Bethesda, MD 20892; [2]Poochon Scientific, Frederick, MD 21704, USA

Abstract. The Cancer Genome Atlas (TCGA) project recently identified the importance of mutations in chromatin remodeling genes in human carcinomas. These findings imply that epigenetic modulators might have a therapeutic role in urothelial cancers. To exploit histone deacetylases (HDACs) as targets for cancer therapy, we investigated the HDAC inhibitors (HDACIs) romidepsin, trichostatin A, and vorinostat as potential chemotherapeutic agents for bladder cancer. We demonstrate that the three HDACIs suppressed cell growth and induced cell death in the bladder cancer cell line 5637. To identify potential mechanisms associated with the anti-proliferative and cytotoxic effects of the HDACIs, we used quantitative proteomics to determine the proteins potentially involved in these processes. Our proteome studies identified a total of 6003 unique proteins. Of these, 2472 proteins were upregulated and 2049 proteins were downregulated in response to HDACI exposure compared to the untreated controls (P<0.05). Bioinformatic analysis further revealed that those differentially expressed proteins were involved in multiple biological functions and enzyme-regulated pathways, including cell cycle progression, apoptosis, autophagy, free radical generation and DNA damage repair. HDACIs also altered the acetylation status of histones and non-histone proteins, as well as the levels of chromatin modification proteins, suggesting that HDACIs exert multiple cytotoxic actions in bladder cancer cells by inhibiting HDAC activity or altering the structure of chromatin. We conclude that HDACIs are effective in the inhibition of cell proliferation and the induction of apoptosis in the 5637 bladder cancer cells through multiple cell death-associated pathways. These observations support the notion that HDACIs provide new therapeutic options for bladder cancer treatment and thus warrant further preclinical exploration.

Introduction

Urinary bladder cancer is the second most common malignant tumor of the genitourinary tract and ranks fourth among male cancers (1). Approximately 70% of initially diagnosed tumors are superficial and can be treated by transurethral resection, while the remaining 30% become muscle invasive and are associated with a high risk of metastatic disease (2,3). Systemic chemotherapy is a treatment option for patients with locally advanced or metastatic disease. Despite huge efforts to tackle the disease in the past two decades, current treatments confer only a modest survival benefit upon bladder cancer patients, and long-term survival of patients suffering from metastatic disease does not exceed 20% (4); therefore, there is an urgent need for innovative ideas that deviate from conventional approaches.

The search for novel chemical agents against cancer has long been the mainstay of cancer research. During recent years, it has been shown that epigenetic aberrations are involved in tumorigenesis. Particularly, an imbalance in the equilibrium between histone acetylation and histone deacetylation has been proposed as a driving force, causing normal cells to become malignant. Therefore, modulating acetylation may be an innovative strategy to treat malignant disease. Acetylation is catalyzed by a specific enzyme family, histone acetyltransferases (HATs), and correlates with nucleosome remodeling and transcriptional activation, whereas deacetylation of histone tails is catalyzed by histone deacetylases (HDACs) and induces transcriptional repression through chromatin condensation (5).

Altered expression of different HDACs has been reported in various human cancers (6-12). Systemic analysis of the expression levels of HDACs in cultured cancer cell lines, as well as primary cultures of human cancer cells and various human tumor biopsy samples, frequently identifies higher levels of

---

Correspondence to: Dr Qingdi Quentin Li or Dr Piyush K. Agarwal, National Institutes of Health, Bethesda, MD 20892, USA
E-mail: liquenti@mail.nih.gov
E-mail: agarwalpk2@mail.nih.gov

expression than in corresponding normal tissue. For instance, recent evidence shows that both clinical samples from patients with urinary bladder cancer and tumor tissues from a mouse model have demonstrated a significantly increased HDAC expression compared with surrounding healthy tissue (13). Thus, HDAC inhibition might be an effective option to treat bladder cancer.

Thus far, 18 HDACs have been identified in mammals that are classified into four classes based on their homology to yeast proteins (7,14). Class I HDAC enzymes (HDACs 1, 2, 3 and 8) are widely expressed (12,15), class II HDAC enzymes (HDACs 4, 5, 6, 7, 9 and 10) have tissue-specific distribution and are involved in organ development and function (12), and other classes are less specific in terms of tissue distribution and function. HDAC inhibitors (HDACIs) prevent HDACs from removing acetyl groups, leading to increased acetylation and allowing DNA to remain transcriptionally active (5). There are many known natural and synthetic HDACIs, which can be subdivided into five structural classes, including hydroxamates, cyclic peptides, aliphatic acids, benzamines and electrophilic ketones. The hydroxamate compound trichostatin A (TSA) is a potent nanomolar inhibitor of most class I and class II HDAC enzymes (12,16). Romidepsin (FK228) is the only cyclic peptide HDACI in clinical development (17,18), and it potently inhibits class I HDACs (12,18). Class I HDAC enzymes are overexpressed in many malignancies, and this overexpression is often associated with poor prognosis (12). A number of structurally different HDACIs are in clinical trials for a wide variety of hematologic and solid neoplasms, including cancer of the lung, breast, pancreas, and kidney, melanoma, glioblastoma, leukemias, lymphomas and multiple myeloma (5). Among them, romidepsin and vorinostat (SAHA) have been approved by the Food and Drug Administration for the treatment of cutaneous T-cell lymphoma (CTCL). However, the effect and the mechanism of action of HDACIs as chemotherapeutic regimens for bladder cancer remain to be determined.

Herein, we show that the treatment with HDACIs (romidepsin, TSA and SAHA) inhibited cell growth and proliferation in a dose-dependent fashion in the urinary bladder cancer cell line 5637. We further analyzed the protein expression patterns in response to romidepsin and TSA in this cell model system using quantitative proteomic studies and found that the effect of these two HDACIs on growth inhibition and cell death is mediated through modulating the expression of proteins involved in cell cycle progression, apoptosis, autophagy, reactive oxygen species (ROS) generation and DNA damage repair in 5637 bladder cancer cells.

Materials and methods

Chemicals and reagents. The minimum essential medium (MEM), fetal bovine serum (FBS), penicillin-streptomycin (100X), and 0.25% trypsin-EDTA solution (1X) were obtained from Invitrogen Corp., Life Technologies (Carlsbad, CA, USA). Trichostatin A (TSA) (>98% purity) was from Selleckchem (Houston, TX, USA). Romidepsin (FK228) (>98% purity) was purchased from Apexbio Technology LLC (Houston, TX, USA). Vorinostat (SAHA) and dimethyl sulfoxide (DMSO) were from Sigma-Aldrich (St. Louis, MO, USA). Romidepsin,

TSA or SAHA were dissolved in DMSO separately and stored at -20˚C. The CellTiter 96 AQueous One Solution Cell Proliferation Assay was from Promega Corp. (Madison, WI, USA).

Cell culture and cell viability assay. The human bladder cancer cell line 5637 was purchased from the American Type Culture Collection (ATCC; Manassas, VA, USA). The cell line was grown in MEM, supplemented with 10% FBS, 50 IU/ml penicillin, and 50 μg/ml streptomycin, at 37˚C in a humidified atmosphere with 5% CO_2.

The antiproliferative effects of romidepsin, TSA and SAHA were assessed using an MTS (3-(4,5-dimethylthiazol-2-yl)-5-(3-carboxymethoxyphenyl)-2-(4-sulfophenyl)-2H-tetrazolium)-based assay (Promega) as previously described (19). In brief, 5637 bladder carcinoma cells ($5x10^3$ cells/well) were evenly distributed in 96-well plates, grown overnight, and then treated with various concentrations of romidepsin, TSA or SAHA at the indicated concentrations (0, 0.1 1, 10 and 100 nM, 1, 10 and 100 μM) for 24 or 72 h. At the end of incubation, 20 μl of CellTiter 96 AQueous One Solution reagent was added to each well of the assay plates containing the treated and untreated cells in 200 μl of culture medium, and the plates were incubated at 37˚C and 5% CO_2 for 2 h. The optical density at 490 nm was determined using a 96-well iMark™ Microplate reader (Bio-Rad Laboratories, Hercules, CA, USA). Proliferation rates were calculated from the optical densities of the HDACI-treated cells relative to the optical density of DMSO-treated control cells with no HDACI exposure (control value, 100%). The half-maximal inhibitory concentration (IC_{50}) values for romidepsin, TSA and SAHA on 24 and 72 h in 5637 cell line were calculated using GraphPad Prism version 6.01 software (GraphPad Software, Inc., La Jolla, CA, USA). IC_{50} was considered as the drug concentration that decreases the cell count by 50%. Non-linear regression curve fitting was performed. The data were fitted to an exponential first-order decay function.

Preparation of protein extraction, separation of proteins and in-gel trypsin digestion. Total protein extraction from cell pellets was prepared by the following method. In brief, cell pellets were lysed in 0.4 ml lysis buffer (20 mM Tris-HCl, pH 7.5, 150 mM NaCl, 1 mM Na_2EDTA, 1 mM EGTA, 1% Triton X-100, protease inhibitor cocktail pill). After cells were lysed, 50 μl of 10% SDS and 50 μl of 1 M DTT were added into the mixture followed by incubation at 95˚C for 10 min. The extraction was then sonicated and centrifuged at 15,000 x g for 10 min. Supernatants were collected and stored at -80˚C for further analysis. The protein concentration of the supernatants was determined by a BCA™ reducing reagent compatible assay kit (Thermo Fisher Scientific, Rockford, IL, USA).

Equal amounts of protein (130 μg) from each sample were fractioned by separation on a NuPAGE 4-12% Bis-Tris Gel (Life Technologies, Grand Island, NY, USA). Sixteen gel fractions from each lane representing one sample were treated with DTT for reduction, then iodoacetamide for alkylation, and further digested by trypsin in 25 mM NH_4HCO_3 solution. The digested protein was extracted, and the extracted peptides were dried and reconstituted in 20 μl of 0.1% formic acid before nanospray LC/MS/MS analysis was performed.

Nanospray LC/MS/MS analysis. Sixteen tryptic peptide fractions from one cell sample were analyzed sequentially using a Thermo Scientific Q Exactive Hybrid Quadrupole-Orbitrap mass spectrometer equipped with a Thermo Dionex UltiMate 3000 RSLCnano system. Tryptic peptide samples were loaded onto a peptide trap cartridge at a flow rate of 5 μl/min. The trapped peptides were eluted onto a reversed-phase 25-cm C18 Picofrit column (New Objective, Woburn, MA, USA) using a linear gradient of acetonitrile (3-36%) in 0.1% formic acid. The elution duration was 110 min at a flow rate of 0.3 μl/min. Eluted peptides from the Picofrit column were ionized and sprayed into the mass spectrometer, using a Nanospray Flex Ion Source ES071 (Thermo Fisher Scientific) under the following settings: spray voltage, 1.6 kV and capillary temperature, 250˚C. The Q Exactive instrument was operated in the data dependent mode to automatically switch between full scan MS and MS/MS acquisition. Survey full scan MS spectra (m/z 300-2000) was acquired in the Orbitrap with 70,000 resolution (m/z 200) after accumulation of ions to a 3×10^6 target value based on predictive AGC from the previous full scan. Dynamic exclusion was set to 20 sec. The 12 most intense multiply-charged ions (z ≥2) were sequentially isolated and fragmented in the Axial higher energy collision-induced dissociation (HCD) cell using normalized HCD collision energy at 25% with an AGC target 1e5 and a maxima injection time of 100 ms at 17,500 resolution.

LC/MS/MS data analysis. The raw MS files were analyzed using the Thermo Proteome Discoverer 1.4.1 platform (Thermo Fisher Scientific, Bremen, GmbH) for peptide identification and protein assembly. For each cell sample, 16 raw MS files obtained from 16 sequential LC/MS analyses were grouped for a single database search against the Human UniProtKB/Swiss-Prot human protein sequence databases (20597 entries, 12/20/2013) based on the SEQUEST and percolator algorithms through the Proteome Discoverer 1.4.1 platform. Carbamidomethylation of cysteines was set as a fixed modification. The minimum peptide length was specified to be five amino acids. The precursor mass tolerance was set to 15 ppm, whereas fragment mass tolerance was set to 0.05 kDa. The maximum false peptide discovery rate was specified as 0.01. The resulting Proteome Discoverer Report contains all assembled proteins (a proteome profile) with peptides sequences and matched spectrum counts. Three proteome profiles were generated for the untreated control cells and two HDACI-treated cell samples.

Protein quantification. Protein quantification used the normalized spectral abundance factors (NSAFs) method to calculate the protein relative abundance (20,21). To quantitatively describe the relative abundance, the ppm (part per million) was chosen as the unit and the 1,000,000 ppm value was assigned to each proteome profile. A ppm value at the range of 0-1,000,000 ppm for each identified protein in each proteome profile was calculated based on its normalized NSAF.

The ppm was calculated as follows: $RC_N = 10^6 \times NSAF_N$, where RC_N is the relative concentration of protein N in the proteome of test sample, $NSAF_N$ is the protein's normalized spectral abundance factor and N is the protein index.

NSAFs were calculated as follows: $NSAF_N = (S_N/L_N)/(\Sigma_{ni=1}S_i/L_i)$, where N is the protein index, S_N is the number of peptide spectra matched to the protein, L_N is the length of protein N (number of amino acid residues), and n is the total number of proteins in the input database (proteome profile for one cell sample). The ratio of HDACI treated vs. untreated control was defined as 1,000 if the protein was not identified in untreated control, or as 0.001 if the protein was not identified in HDACI-treated sample.

Signaling pathway analysis. The cell functions are executed and regulated by the entire sets of proteins (the proteome). The regulation of different cellular functions has been categorized into a number of pathways, such as cell cycle and apoptosis signaling pathways. In each pathway, the components according to their functions are generally named as ligands, receptors, activating regulators, inhibitory regulators and effectors. In order to measure the activation strength of a pathway, the protein molecules that belong to ligands, receptors, activating regulators, inhibitory regulators, or effectors were grouped and their relative abundances (ppm) were summed. The protein list for all analyzed pathways and processes was obtained from the Kyoto Encyclopedia of Genes and Genomes (KEGG) pathway database (http://www.genome.jp/kegg/pathway.html), and their functional annotations were manually confirmed using the UniProtKB protein database and the NCBI protein database or available publications.

Statistical data analysis. All quantitative values are presented as means ± SD. Data were statistically analyzed using two-way analysis of variance (ANOVA) for comparison among groups. Student's t-test was used to analyze the statistical significance of differences between untreated controls and HDACI-treated groups. All P-values were determined using a two-sided test, and P-values <0.05 were considered to indicate significance.

Results

HDACIs inhibit cell proliferation and induce cytotoxicity in human bladder cancer cells. To investigate the effect of HDACIs on bladder cancer cell growth and proliferation, we selected human bladder cancer 5637 cells, a cell line commonly used as a model for studying bladder carcinoma. The dose-response of romidepsin, TSA and SAHA inhibition of the growth of 5637 cell line was characterized *in vitro* using the MTS assay. Romidepsin, TSA or SAHA at concentrations of 0.1 nM to 100 μM caused dose-dependent inhibition of the proliferation of 5637 cells at 72 h (Fig. 1A). The half-maximal inhibitory concentration (IC_{50}) values of romidepsin, TSA and SAHA at 72 h in this line were 1.0±0.1 nM, 100±3.5nM and 1.9±0.1 μM, respectively. These results indicate that HDACIs can potently inhibit cell proliferation and induce cell toxicity in bladder cancer cells.

Previous study has demonstrated that HDACIs increase histone acetylation levels in human bladder cancer cells and that these levels peak at 24 h and decrease gradually over 48-72 h (22). Therefore, we chose 24-h treatment with HDACIs for this *in vitro* study. To establish the appropriate HDACI treatment concentration for our proteomic studies, we performed cytotoxicity assays in 5637 cells in response to romidepsin,
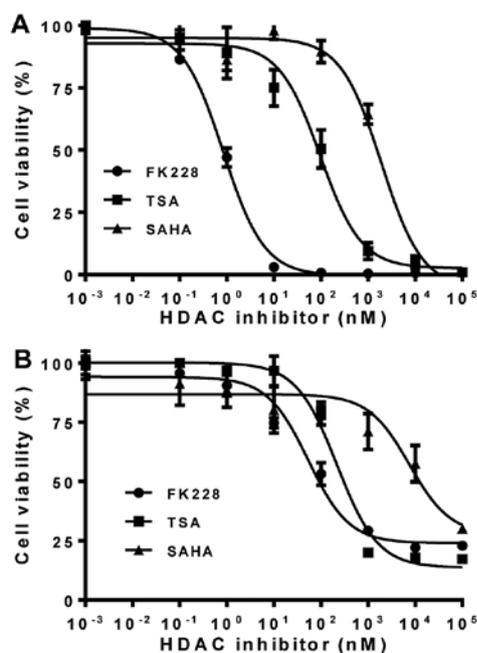
Figure 1. Histone deacetylase inhibitors (HDACIs) suppress cell proliferation and induce cytotoxicity in human bladder cancer 5637 cells. Cells (5637) were evenly distributed in 96-well plates (5×10^3 cells/well) and treated for 72 h (A) or 24 h (B) with romidepsin (FK228), trichostatin A (TSA), or vorinostat (SAHA) at the indicated concentrations. The ability of HDACIs to inhibit cell growth and proliferation was determined by the MTS assay, as described in Materials and methods. Cell viability values are expressed relative to those for cells with no HDACI exposure (control value, 100%). The results represent the means ± SD of three independent experiments. MTS, 3-(4,5-dimethylthiazol-2-yl)-5-(3-carboxymethoxyphenyl)-2-(4-sulfophenyl)-2H-tetrazolium.

TSA or SAHA treatment at different concentrations. As shown in Fig. 1B, with dose-increased HDACI treatment for 24 h, the viability of 5637 cells correspondingly decreased, and the romidepsin, TSA and SAHA working concentrations resulting in 50% cell viability were 50±3.5 nM, 200±20 nM and 7.5±0.5 μM, respectively. Since the activity of romidepsin and TSA was much more potent than SAHA in cytotoxicity in 5637 cells (Fig. 1), we therefore, finally used the working concentrations of 50 and 200 nM for 24-h treatment for romidepsin and TSA, respectively, for the following proteomic experiments.

Quantitative proteomic analysis of bladder cancer cells following HDACI treatment. To analyze the mechanisms responsible for the effect of HDACIs on cell proliferation and cytotoxicity in bladder cancer cells, the whole cell proteome profiles of the HDACI-treated and untreated 5637 cells were compared using quantitative proteomic studies. Differentially expressed proteins were identified and quantified by nanospray LC/MS/MS mass spectrometry. The selection criteria for deregulation were the same for all the samples: identification based on at least two unique peptides and fold difference >2.0 or <-2.0.

Using the nanospray LC/MS/MS analysis, a total of 6003 non-redundant proteins were identified in both HDACI treated and untreated 5637 cells. Of these, 4865, 4618 and 4674 were quantified in romidepsin-treated, TSA-treated and untreated cells, respectively. A total of 3518 proteins were common to the two HDACI-treated cells and untreated cells.

Compared with the untreated control, there were 5698 differentially expressed proteins in romidepsin-treated 5637 cells, including 2969 upregulated proteins (1845 ≥2-fold upregulated proteins) and 2729 downregulated proteins (1626 ≥2-fold downregulated proteins). The fold changes ranged from 45.51 to -35.99 and 1979 of these proteins (both upregulated and downregulated proteins) showed >10-fold deregulation. For the TSA-treated 5637 cells, a total of 5497 proteins were differentially regulated; 2808 were upregulated (1709 ≥2-fold upregulated) and 2689 downregulated (1563 ≥2-fold down-regulated). The fold changes ranged from 36.18 to -26.83 and 1826 of these proteins (both upregulated and downregulated proteins) showed more than 10-fold deregulation. A total of 1082 ≥2-fold upregulated proteins and 1140 ≥2-fold down-regulated proteins were common to both romidepsin-treated and TSA-treated 5637 cells.

Functional classification of differentially expressed proteins in HDACI-treated bladder cancer cells. To gain an initial understanding of the role and function of the identified proteins between the HDACI treated and untreated 5637 bladder cancer cells, we merged the protein datasets and used pathway software to provide a descriptive analysis. The functional correlation analysis of the differentially regulated proteins was done by database search using UniProt, Swiss-Prot and PANTHER. The categorization of differentially expressed proteins (≥2-fold upregulated and downregulated proteins) according to their molecular function, biological process and cellular component is shown in Fig. 2. These data are based on a compilation of proteins from the romidepsin-treated cell samples and are presented to demonstrate the range of molecular functions (Fig. 2A) and biological processes (Fig. 2B) represented by the identified proteins, and the cellular component (Fig. 2C) to which the proteins belong. According to cellular component, the analysis revealed a high percentage of proteins corresponding to the cell part, organelle, macromolecular complex, extracellular region and extracellular matrix (Fig. 2C). Based on molecular function, the most general categories of proteins were catalytic activity, binding activity, structural molecule activity, nucleic acid transcription factor activity, enzyme regulator activity, transporter activity and receptor activity (Fig. 2A). Differentially expressed proteins related to 13 biological processes, including metabolic process, cellular process, localization, biological regulation, developmental process, cellular component organization or biogenesis, response to stimulus and apoptotic process (Fig. 2B).

A majority of the molecular functions and biological processes were affected in both romidepsin-treated and TSA-treated bladder cancer cells. Although romidepsin caused more differentially expressed proteins (3471 ≥2-fold upregulated and downregulated) than those caused by TSA (3272 ≥2-fold upregulated and downregulated proteins), the percentages of proteins in each category of the molecular function and biological process were similar between the romidepsin-treated (Fig. 2A and B) and TSA-treated (data not shown) 5637 cells. There were 1845 and 1709 ≥2-fold upregulated proteins and 1626 and 1563 ≥2-fold downregulated proteins in romidepsin-treated and TSA-treated cell samples, respectively. We also compared and showed that in either the upregulated proteins or the downregulated proteins, there was

A Molecular Function

- Transporter activity (175)
- Translation regulator activity (42)
- Protein binding transcription factor activity (32)
- Enzyme regulator activity (214)
- Catalytic activity (1200)
- Receptor activity (159)
- Nucleic acid binding transcription factor activity (236)
- Antioxidant activity (5)
- Structural molecule activity (285)
- Binding activity (1104)

B Biological Process

- Immune system process (213)
- Cellular component organization or biogenesis (296)
- Cellular process (978)
- Localization (543)
- Apoptotic process (100)
- Reproduction (78)
- Biological regulation (513)
- Response to stimulus (203)
- Developmental process (400)
- Multicellular organismal process (206)
- Locomotion (1)
- Biological adhesion (138)
- Metabolic process (1764)

C Cellular Component

- Synapse (2)
- Cell junction (18)
- Extracellular region (61)
- Membrane (79)
- Macromolecular complex (169)
- Organelle (255)
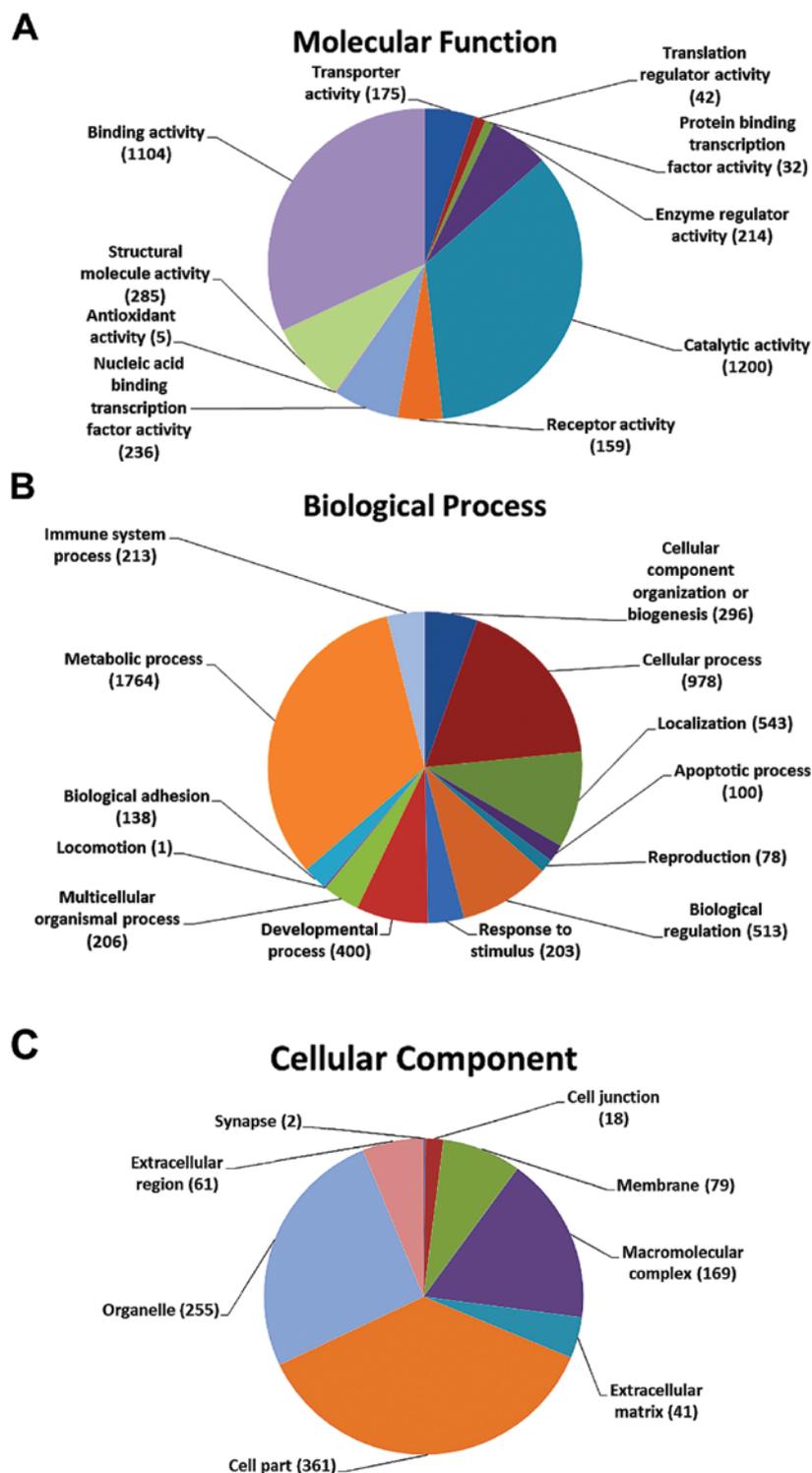- Extracellular matrix (41)
- Cell part (361)

Figure 2. Functional categorization of the proteins that are upregulated and downregulated in romidepsin-treated bladder cancer cells. Differentially regulated proteins were analyzed for 'functional categories' using the UnitProt knowledge database and the PANTHER classification system. The pie charts show the distribution of deregulated proteins (both ≥2-fold upregulated and ≥2-fold downregulated proteins) detected in the romidepsin-treated 5637 cells based on molecular function (A), biological process (B) and cellular component (C). The numbers of the identified and quantified proteins in each category are indicated in parentheses.

no significant difference for the percentages of proteins in each category of the molecular function and biological process between the romidepsin-treated cells and TSA-treated cells (data not shown), suggesting that both romidepsin and TSA exert the same or similar actions on functional categories in our cell model of bladder cancer.

Biological pathway analysis according to the Kyoto Encyclopedia of Genes and Genomes (KEGG). Next, we used KEGG pathway analysis to identify the biological pathways of the proteins that were significantly differentially expressed (≥2-fold upregulated and downregulated) in the HDACI-treated 5637 bladder cancer cells. Pathway analysis using

Table I. Main metabolic and enzymatic pathways associated with the upregulated and downregulated proteins in romidepsin-treated 5637 cells as analyzed by the Kyoto Encyclopedia of Genes and Genomes.[a]

Biological pathway	%	P-value	Benjamini
1845 ≥2-fold upregulated proteins			
Ribosome	1.8	4.0×10^{-9}	7.1×10^{-7}
Oxidative phosphorylation	2.1	5.8×10^{-7}	3.4×10^{-5}
Ubiquitin mediated proteolysis	2.0	6.1×10^{-6}	2.1×10^{-4}
Lysosome	1.5	7.1×10^{-4}	1.5×10^{-2}
Amino sugar and nucleotide sugar metabolism	0.8	1.3×10^{-3}	2.2×10^{-2}
Mismatch repair	0.5	6.8×10^{-3}	8.8×10^{-2}
Basal transcription factors	0.6	7.6×10^{-3}	9.1×10^{-2}
DNA replication	0.6	9.3×10^{-3}	1.0×10^{-2}
Nucleotide excision repair	0.6	3.3×10^{-2}	2.8×10^{-2}
Purine metabolism	1.5	4.1×10^{-2}	3.2×10^{-2}
Pyrimidine metabolism	1.0	6.2×10^{-2}	4.0×10^{-2}
RNA polymerase	0.4	6.2×10^{-2}	3.9×10^{-2}
1626 ≥2-fold downregulated proteins			
N- and O-Glycan biosynthesis	1.3	5.4×10^{-5}	1.2×10^{-4}
Glycerophospholipid metabolism	1.0	4.7×10^{-3}	1.5×10^{-2}
Cell cycle	1.4	4.8×10^{-3}	1.3×10^{-2}
Lysine degradation	0.7	1.1×10^{-2}	2.0×10^{-2}
Valine, leucine and isoleucine degradation	0.6	3.2×10^{-2}	3.8×10^{-2}
Glycerolipid metabolism	0.6	3.6×10^{-2}	3.9×10^{-2}
Sphingolipid metabolism	0.5	4.7×10^{-2}	4.1×10^{-2}
Biosynthesis of unsaturated fatty acids	0.4	3.2×10^{-2}	3.1×10^{-2}
Steroid biosynthesis	0.3	5.3×10^{-2}	4.0×10^{-2}
Bladder cancer	0.5	6.6×10^{-2}	4.1×10^{-2}
Ether lipid metabolism	0.5	7.6×10^{-2}	4.3×10^{-2}
Methane metabolism	0.2	8.8×10^{-2}	4.7×10^{-2}

[a]Similar results were observed in trichostatin A-treated 5637 bladder cancer cells.

KEGG database by DAVID bioinformatics resources tool (DAVID v6.7, the Database for Annotation, Visualization and Integrated Discovery) showed that the downregulated proteins were associated with multiple pathways, such as cell cycle, bladder cancer, lysine degradation, valine, leucine, and isoleucine degradation, and all major annotated lipid metabolism pathways including glycerophospholipid metabolism, steroid biosynthesis, glycerolipid metabolism, sphingolipid metabolism and ether lipid metabolism (Table I). We also performed the same analysis for HDACI upregulated proteins, which were enriched in the DNA replication and nucleotide related processes, including ribosome, amino sugar and nucleotide sugar metabolism, mismatch repair, basal transcription factors, nucleotide excision repair, purine metabolism, pyrimidine metabolism and RNA polymerase (Table I).

HDACI-induced cell death in bladder cancer cells is mediated via modulating cell cycle progression, apoptosis and DNA damage repair. Given that HDACIs have been shown to exert a variety of anticancer activities in different types of tumors and that both romidepsin and TSA induced cell growth inhibition and cell death in our bladder cancer cells (Fig. 1), we elucidated the mechanism underlying the effect of HDACIs on cell proliferation and cytotoxicity in this model system. We performed pathway-clustering analyses of the HDACI-responsive proteome for pathways involved in cell death. The results showed that cell cycle, apoptosis, oxidative stress, autophagy, and DNA damage repair were the most prominent pathways enriched with altered protein levels in HDACI-treated cells (Fig. 3), suggesting that these pathways are involved in HDACI-induced cell death in 5637 bladder cancer cells.

To understand more about the mechanisms of HDACI-induced cell death in our bladder cancer cell model, we identified the differentially expressed proteins related to cell death in these pathways in response to HDACI treatment. Table II shows part of the differentially expressed proteins involved in cell death in both romidepsin and TSA treated cells. These include 37 proteins involved in cell cycle progression, 19 proteins associated with apoptosis process, 30 proteins in various DNA damage repair pathways and 11 proteins involved in ROS generation and autophagy regulation. The functions and levels of the proteins in each pathway are listed in the table.

Table II. Alterations in the levels of the proteins associated with cell death in bladder cancer cells in response to romidepsin or trichostatin A (TSA) treatment.

				Protein level (ppm)		
Accession no.	Protein name	Symbol	Protein function	Untreated	Romidepsin	TSA
Regulation of cell cycle						
116176	G2/mitotic-specific cyclin-B1	CCNB1	Cyclin	7.19	0	0
5921731	G2/mitotic-specific cyclin-B2	CCNB2	Cyclin	7.83	0	0
218511966	Cyclin-K	CCNK	Cyclin	37.57	23.28	7.47
74753368	Cyclin-L1	CCNL1	Cyclin	11.84	6.41	0
9296942	Cyclin-T1	CCNT1	Cyclin	12.87	0	0
6226784	Cyclin-dependent kinase 10	CDK10	CDK	25.95	0	0
205371737	Anaphase-promoting complex subunit 4	APC4	Mitosis factor	15.42	8.36	5.36
37537861	Anaphase-promoting complex subunit 5	APC5	Mitosis factor	4.12	0	0
37537762	Cell division cycle protein 20 homolog	CDC20	Mitosis factor	12.48	0	0
37537763	Cell division cycle protein 16 homolog	CDC16	Mitosis factor	20.09	16.33	0
254763423	Cell division cycle protein 23 homolog	CDC23	Mitosis factor	15.65	0	7.26
12644198	Cell division cycle protein 27 homolog	CDC27	Mitosis factor	7.56	0	0
12230256	Mitotic spindle assembly checkpoint protein MAD2A	MD2L1	Mitosis factor	45.58	0	21.14
729143	Cyclin-dependent kinase inhibitor 1	CDN1A	CDK inhibitor	0	20.58	0
3041660	Cyclin-dependent kinase inhibitor 2A	CD2A1	CDK inhibitor	59.89	173.11	55.56
172047302	Cyclin-D1-binding protein 1	CCNDBP1	CDK inhibitor	0	9.38	12.04
1709658	Serine/threonine-protein kinase PLK1	PLK1	Positive regulator	30.99	5.60	0
68571766	DNA replication licensing factor MCM4	MCM4	Positive regulator	21.65	7.82	15.06
19858646	DNA replication licensing factor MCM5	MCM5	Positive regulator	67.89	59.79	59.04
76803807	Origin recognition complex subunit 1	ORC1	Positive regulator	7.23	3.92	5.03
6174924	Origin recognition complex subunit 5	ORC5	Positive regulator	21.48	7.76	19.92
25091097	Double-strand-break repair protein rad21 homolog	RAD21	Positive regulator	167.81	32.10	27.47
13633914	Mothers against decapentaplegic homolog 2	SMAD2	Positive regulator	13.34	7.23	9.28
51338669	Mothers against decapentaplegic homolog 3	SMAD3	Positive regulator	51.29	7.94	10.20
29336622	Structural maintenance of hromosomes protein 1A	SMC1A	Positive regulator	434.44	177.95	207.35
29337005	Structural maintenance of chromosomes protein 3	SMC3	Positive regulator	442.71	183.07	188.71
209572720	Cohesin subunit SA-1	STAG1	Positive regulator	17.33	10.73	3.44
73621291	Cohesin subunit SA-2	STAG2	Positive regulator	43.01	10.97	0
135674	Transforming growth factor β-1	TGFB1	Positive regulator	23.96	0	0
132164	Retinoblastoma-associated protein	RB	Positive regulator	3.36	0	0
1345590	14-3-3 protein β/α	YWHAB	Negative regulator	468.41	644.94	827.91
51702210	14-3-3 protein ε	YWHAE	Negative regulator	708.35	1006.08	1053.59
1345593	14-3-3 protein η	YWHAH	Negative regulator	215.22	343.05	563.68
48428721	14-3-3 protein γ	YWHAG	Negative regulator	428.69	464.67	719.29
112690	14-3-3 protein θ	YWHAQ	Negative regulator	483.03	771.58	937.41
52000887	14-3-3 protein ζ/δ	YWHAZ	Negative regulator	699.13	771.58	1025.84
398953	14-3-3 protein σ	SFN	Negative regulator	452.08	476.40	698.92

Table II. Continued.

Accession no.	Protein name	Symbol	Protein function	Protein level (ppm)		
				Untreated	Romidepsin	TSA
Regulation of apoptosis						
6094511	Tumor necrosis factor receptor type 1-associated DEATH domain protein	TRADD	Pro-apoptosis	0	10.82	0
20141188	Apoptotic protease-activating factor 1	APAF	Pro-apoptosis	0	5.41	0
18203316	Diablo homolog, mitochondrial	DBLOH	Pro-apoptosis	195.46	211.86	253.83
17376879	Serine protease HTRA2, mitochondrial	HTRA2	Pro-apoptosis	54.40	73.70	75.69
728945	Apoptosis regulator BAX	BAX	Pro-apoptosis	97.32	351.63	203.12
2493274	Bcl-2 homologous antagonist/killer	BAK	Pro-apoptosis	29.52	63.99	41.07
2493285	BH3-interacting domain death agonist	BID	Pro-apoptosis	31.94	207.73	88.89
23396740	Bcl-2-like protein 13	B2L13	Pro-apoptosis	12.84	20.88	26.80
2810997	DNA fragmentation factor subunit α	DFFA	Pro-apoptosis	9.41	40.79	39.27
575773389	Serine-protein kinase ATM	ATM	Pro-apoptosis	1.02	1.10	2.84
77416852	Caspase-3	CASP3	Caspase	11.24	24.37	46.93
115612	Calpain small subunit 1	CPNS1	Calpain-calcium	81.34	151.15	129.35
62906858	Interleukin-1 β	IL1B	Pro-survival	46.31	0	16.11
125987833	Interleukin-1 receptor-associated kinase-like 2	IRAK2	Pro-survival	14.95	0	0
18202671	Myeloid differentiation primary response protein MyD88	MYD88	Pro-survival	10.52	0	0
21542418	Nuclear factor NF-kappa-B p105 subunit	NFKB1	Pro-survival	9.65	0	0
125193	cAMP-dependent protein kinase type I-α regulatory subunit	PRKAR1A	Pro-survival	147.13	8.86	34.12
229463042	cAMP-dependent protein kinase type I-β regulatory subunit	PRKAR1B	Pro-survival	32.70	0	0
125198	cAMP-dependent protein kinase type II-α regulatory subunit	PRKAR2A	Pro-survival	92.50	75.20	85.81
Regulation of DNA damage repair						
73921676	DNA-(apurinic or apyrimidinic site) lyase 2	APEX2	Base excision repair	12.02	0	0
251757259	DNA ligase 3	LIG3	Base excision repair	37.04	23.42	17.18
317373290	DNA repair protein XRCC1	XRCC1	Base excision repair	49.20	16.00	41.07
130781	Poly [ADP-ribose] polymerase 1	PARP1	Base excision repair	380.84	236.36	311.96
17380230	Poly [ADP-ribose] polymerase 2	PARP2	Base excision repair	26.71	5.79	0
296453081	DNA repair protein complementing XP-C cells	XPC	Nucleotide excision repair	3.31	0	0
12643730	DNA damage-binding protein 1	DDB1	Nucleotide excision repair	188.50	109.56	148.24
12230033	DNA damage-binding protein 2	DDB2	Nucleotide excision repair	29.17	0	10.15
119541	TFIIH basal transcription factor complex helicase XPB subunit	ERCC3	Nucleotide excision repair	31.86	17.27	11.08
17380326	General transcription factor IIH subunit 2	GTF2H2	Nucleotide excision repair	31.54	8.55	0
50403772	General transcription factor IIH subunit 3	GTF2H3	Nucleotide excision repair	30.33	21.92	14.07
17380328	General transcription factor IIH subunit 4	GTF2H4	Nucleotide excision repair	74.15	7.31	56.28

Table II. Continued.

| Accession no.	Protein name	Symbol	Protein function	Protein level (ppm)		
				Untreated	Romidepsin	TSA
1706232	Cyclin-H	CCNH	Nucleotide excision repair	28.93	10.45	26.83
25091548	Pre-mRNA-splicing factor SYF1	XAB2	Nucleotide excision repair	87.42	51.33	35.48
108936013	Cullin-4A	CUL4A	Nucleotide excision repair	36.93	22.24	22.84
60392986	DNA repair protein RAD50	RAD50	Homologous recombination	71.21	51.46	36.33
17380137	Double-strand break repair protein MRE11A	MRE11A	Homologous recombination	39.59	4.77	24.48
74762960	Nibrin	NBN	Homologous recombination	41.30	13.4	5.75
116242745	DNA endonuclease RBBP8	RBBP8	Homologous recombination	3.47	0	0
166898077	Crossover junction endonuclease MUS81	MUS81	Homologous recombination	5.65	0	0
2501242	DNA topoisomerase 3-α	TOP3A	Homologous recombination	3.11	0	0
38258929	DNA-dependent protein kinase catalytic subunit	PRKDC	Non-homologous end-joining	521.31	295.21	363.21
125731	X-ray repair cross-complementing protein 5	XRCC5	Non-homologous end-joining	582.87	387.37	443.99
125729	X-ray repair cross-complementing protein 6	XRCC6	Non-homologous end-joining	772.18	454.52	619.04
74760390	WD repeat-containing protein 48	WDR48	Fanconi anemia	4.60	0	0
48428038	Aprataxin	APTX	Editing and processing nuclease	43.74	0	0
146325723	E3 ubiquitin-protein ligase SHPRH	SHPRH	Ubiquitination and modification	1.85	0	0
68565701	Telomere-associated protein RIF1	RIF1	Other related	51.65	15.02	8.76
1705919	Dual specificity protein kinase CLK2	CLK2	Other related	12.48	0	0
55976619	Pre-mRNA-processing factor 19	PRPF19	Other related	463.44	241.12	335.32
ROS generation						
14916998	Glutathione reductase	GSHR	Reductase	17.90	6.47	8.30
182705230	Thioredoxin reductase 2	TRXR2	Reductase	17.83	0	0
2506326	Xanthine dehydrogenase/oxidase	XDH	Oxidase	0	2.67	2.53
Regulation of autophagy						
254763436	Protein kinase, AMP-activated, α 1 catalytic subunit	PRKAA1	Autophagy	22.28	36.23	46.51
20178289	Interferon, α 21	IFNA21	Autophagy	0	17.86	0
74762700	Phosphoinositide-3-kinase, regulatory subunit 4	PIK3R4	Autophagy	0	4.97	3.19
74730233	Phosphatidylinositol 3-kinase, catalytic subunit type 3	PIK3C3	Autophagy	0	3.81	4.89
62286592	Autophagy related 7	ATG	Autophagy	22.15	62.42	12.33
62510482	Autophagy related 16-like 1 (*S. cerevisiae*)	ATG16L1	Autophagy	5.13	11.12	0
44888808	GABA(A) receptor-associated protein-like 2	GABARAPL	Autophagy	0	28.85	111.11
61212142	Autophagy related 3	ATG3	Autophagy	0	10.75	55.20

ROS, reactive oxygen species.
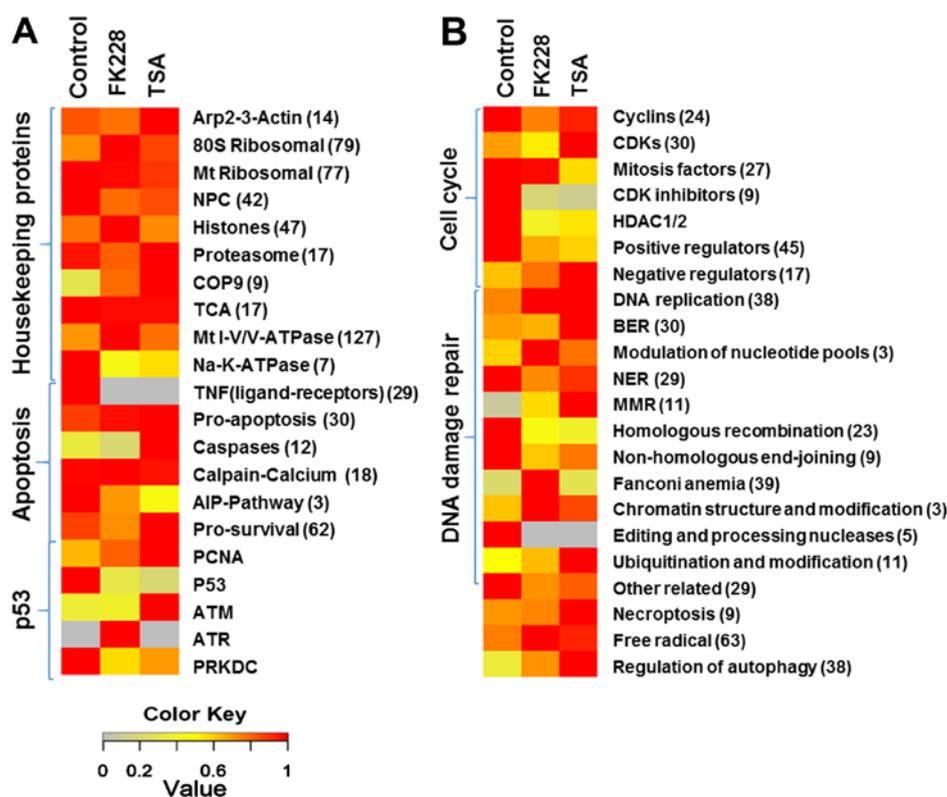
Figure 3. Protein expression profile of the bladder cancer 5637 cells treated with romidepsin (FK228) and trichostatin A (TSA). Heat map showing clustering analysis of the proteins with altered expression based on cellular pathways in FK228 or TSA treated 5637 cells compared to those of the untreated control cells. Proteins were annotated based on the Kyoto Encyclopedia of Genes and Genomes pathway database. (A) Heat map showing the identified and quantified housekeeping proteins and the proteins in p53 and apoptosis pathways. (B) Heat map showing the identified and quantified proteins in DNA damage repair, cell cycle regulation, necroptosis, free radical generation and autophagy pathways. The numbers of the identified and quantified proteins in each category are shown in parentheses. The indicated color scale is based on relative quantifications (ppm) assigning the highest ppm as 1. Gray, signal was not detected.

Table III. Histone deacetylase inhibitors induce enhanced global lysine acetylation in histones and non-histone proteins in 5637 bladder cancer cells as determined by proteomic analysis.

Treatment	Histone protein	Non-histone protein
Untreated	172	426
Romidepsin	422	841
Trichostatin A	280	638

For example, our data showed that multiple autophagy-associated proteins, such as ATG3, PRKAA1, GABARAPL and ATG7, were highly upregulated (Table II), suggesting that these proteins might have important roles in HDACI-induced autophagy in bladder carcinoma.

HDACIs enhance global histone and non-histone protein acetylation levels and induce deregulation of chromatin modification proteins. Since both romidepsin and TSA are HDACIs, we assessed the effect of the two HDACIs on lysine acetylation in 5637 cells. We first verified whether inhibition of histone deacetylation by the HDACIs altered global acetylation in our model system. We searched the whole cell proteome and identified the non-redundant peptides containing the acetylated lysine residues. As shown in Table III, both romidepsin and TSA significantly increased global histone and non-histone lysine acetylation levels compared to the untreated control. Romidepsin induced ~2.5-fold and 2-fold increases in histone and non-histone protein acetylation levels, respectively ($P<0.01$), while TSA increased global lysine acetylation levels 63 and 50% in histone and non-histone proteins, respectively ($P<0.05$), indicating that romidepsin exerts a more potent effect than TSA on the lysine acetylated profile of both non-histone substrates and core histones in 5637 cells.

Next, the overall increased lysine acetylation levels in histone proteins prompted us to further investigate the impact of HDACIs on site-specific histone lysine acetylation. To this end, we applied the quantitative proteomics to profile histone lysine acetylation in 5637 cells after romidepsin or TSA treatment, followed by protein sequence database search for peptide identification and post-translational modification site mapping. The diagram of Fig. 4 shows that a total of 23 lysine acetylation (Kac) sites in core histones were identified, in most of them Kac sites were previously reported in core histones in mammalian cells. Importantly, we identified two new histone marks, including H2AK118ac and H2BK34ac in both romidepsin and TSA treated 5637 cells (Fig. 4A and B). The representative spectra of histone lysine acetylated peptides are shown in Fig. 4C and D, including the spectra for peptides of H2AK118ac and H2BK34ac. In addition, the sequences of
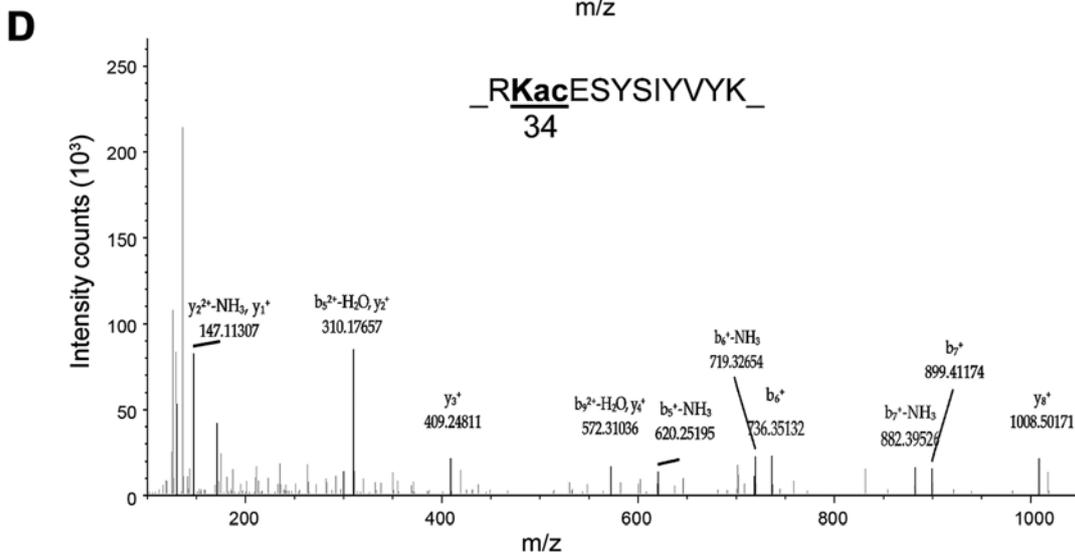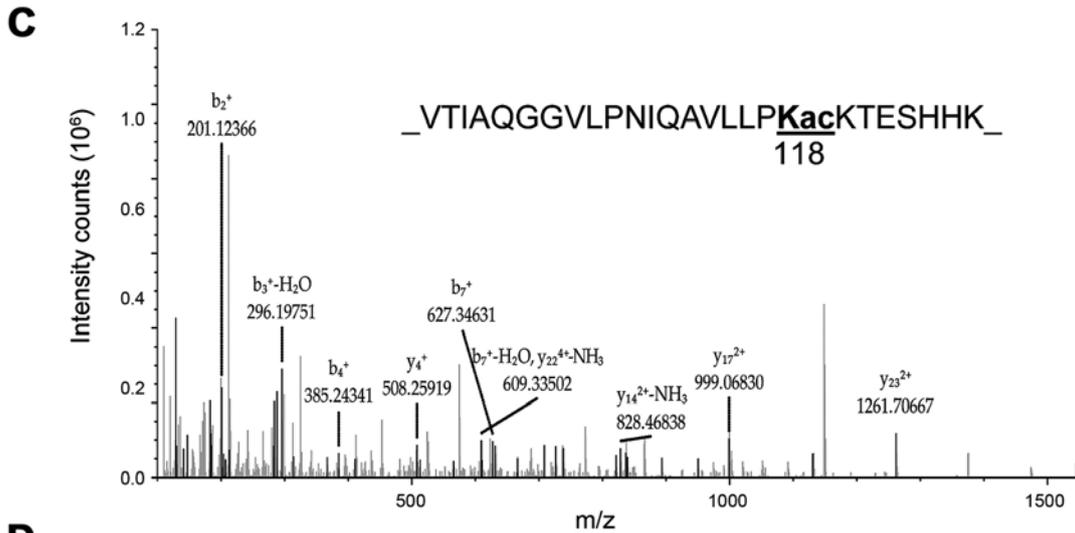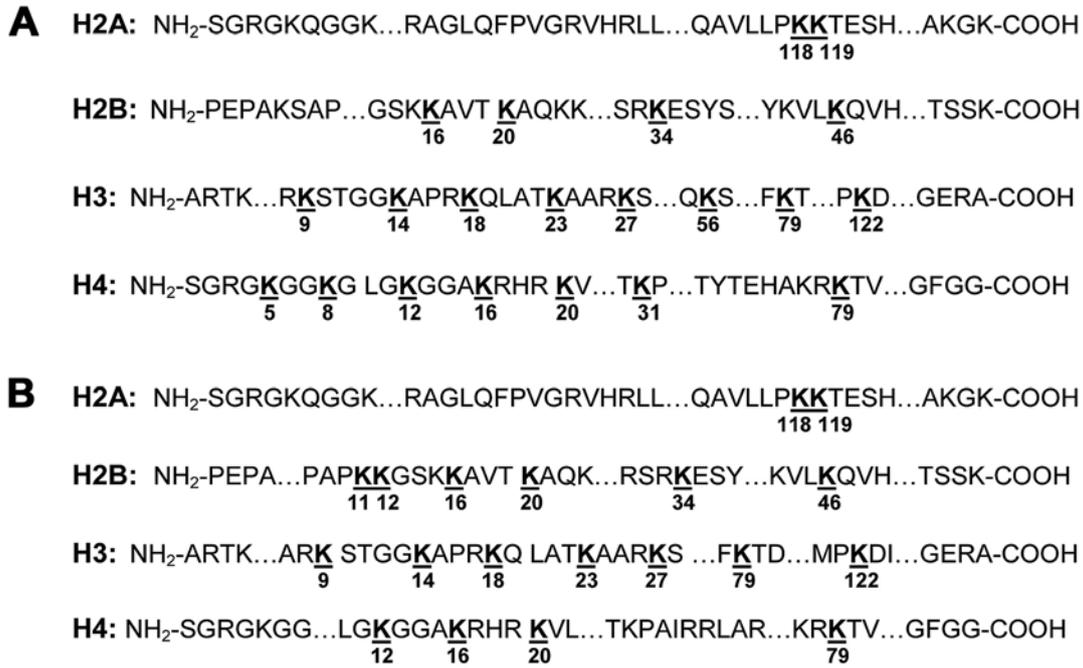
A **H2A:** NH$_2$-SGRGKQGGK...RAGLQFPVGRVHRLL...QAVLLP**KK**TESH...AKGK-COOH
118 119

H2B: NH$_2$-PEPAKSAP...GSK**K**AVT **K**AQKK...SR**K**ESYS...YKVL**K**QVH...TSSK-COOH
16 **20** **34** **46**

H3: NH$_2$-ARTK...R**K**STGG**K**APR**K**QLAT**K**AAR**K**S...Q**K**S...F**K**T...P**K**D...GERA-COOH
9 **14** **18** **23** **27** **56** **79** **122**

H4: NH$_2$-SGRG**K**GG**K**G LG**K**GGA**K**RHR **K**V...T**K**P...TYTEHAKR**K**TV...GFGG-COOH
5 **8** **12** **16** **20** **31** **79**

B **H2A:** NH$_2$-SGRGKQGGK...RAGLQFPVGRVHRLL...QAVLLP**KK**TESH...AKGK-COOH
118 119

H2B: NH$_2$-PEPA...PAP**KK**GSK**K**AVT **K**AQK...RSR**K**ESY...KVL**K**QVH...TSSK-COOH
11 12 **16** **20** **34** **46**

H3: NH$_2$-ARTK...AR**K** STGG**K**APR**K**Q LAT**K**AAR**K**S ...F**K**TD...MP**K**DI...GERA-COOH
9 **14** **18** **23** **27** **79** **122**

H4: NH$_2$-SGRGKGG...LG**K**GGA**K**RHR **K**VL...TKPAIRRLAR...KR**K**TV...GFGG-COOH
12 **16** **20** **79**

C _VTIAQGGVLPNIQAVLLP**Kac**KTESHHK_
118

b$_2$$^+$ 201.12366
b$_3$$^+$-H$_2$O 296.19751
b$_4$$^+$ 385.24341
y$_4$$^+$ 508.25919
b$_7$$^+$ 627.34631
b$_7$$^+$-H$_2O, y_{22}$$^{4+}$-NH$_3$ 609.33502
y$_{14}$$^{2+}$-NH$_3$ 828.46838
y$_{17}$$^{2+}$ 999.06830
y$_{23}$$^{2+}$ 1261.70667

D _R**Kac**ESYSIYVYK_
34

y$_2$$^{2+}$-NH$_3$, y$_1$$^+$ 147.11307
b$_5$$^{2+}$-H$_2O, y_2$$^+$ 310.17657
y$_3$$^+$ 409.24811
b$_7$$^{2+}$-H$_2O, y_4$$^+$ 572.31036
b$_5$$^+$-NH$_3$ 620.25195
b$_6$$^+$-NH$_3$ 719.32654
b$_6$$^+$ 736.35132
b$_7$$^+$-NH$_3$ 882.39526
b$_7$$^+$ 899.41174
y$_8$$^+$ 1008.50171

Figure 4. Identification and quantitation of lysine acetylation in core histones of the 5637 bladder cancer cells. The illustration of identified lysine acetylation sites in core histones in the 5637 cells in response to romidepsin (A) and trichostatin A (B) exposure. The identified acetylation sites in core histones are numbered and underlined. (C) MS/MS spectra of a tryptic peptide histone H2AK118 acetylated peptide _VTIAQGGVLPNIQAVLLPK(ac)K(ac)TESHHK_ and (D) MS/MS spectra of a tryptic peptide histone H2BK34 acetylated peptide _ RK(ac)ESYSIYVYK_.

Table IV. The identified lysine acetylation (Kac) sites in core histones and the lysine-acetylated peptide sequences in histone deacetylase inhibitor-treated bladder cancer 5637 cells.

Modified histone site	Modified peptide sequence
Romidepsin treatment	
H2AK118ac	_VTIAQGGVLPNIQAVLLPK(ac)K(ac)TESHHK_
H2AK119ac	_VTIAQGGVLPNIQAVLLPK(ac)K(ac)_
H2BK16ac	_K(ac)AVTK(ac)AQK_
H2BK20ac	_K(ac)AVTK(ac)AQK_
H2BK34ac	_K(ac)ESYSIYVYK_
H2BK46ac	_VLK(ac)QVHPDTGISSK_
H3K9ac	_K(ac)STGGK(ac)APR_
H3K14ac	_K(ac)STGGK(ac)APR_
H3K18ac	_K(ac)QLATK(ac)AAR_
H3K23ac	_K(ac)QLATK(ac)AAR_
H3K27ac	_K(ac)SAPATGGVKKPHR_
H3K56ac	_YQK(ac)STELLIR_
H3K79ac	_EIAQDFK(ac)TDLR_
H3K122ac	_VTIMPK(ac)DIQLAR_
H4K5ac	_GK(ac)GGK(ac)GLGK_
H4K8ac	_GK(ac)GGK(ac)GLGK_
H4K12ac	_GLGK(ac)GGAK(ac)R_
H4K16ac	_GLGK(ac)GGAK(ac)R_
H4K20ac	_K(ac)VLRDNIQGITKPAIR_
H4K31ac	_DNIQGITK(ac)PAIR_
H4K79ac	_K(ac)TVTAMDVVYALKR_
Trichostatin A treatment	
H2AK118ac	_VTIAQGGVLPNIQAVLLPK(ac)K(ac)TESHHK_
H2AK119ac	_VTIAQGGVLPNIQAVLLPK(ac)K(ac)_
H2BK11ac	_SAPAPK(ac)K(ac)GSK_
H2BK12ac	_SAPAPK(ac)K(ac)GSK_
H2BK16ac	_K(ac)AVTK(ac)AQK_
H2BK20ac	_K(ac)AVTK(ac)AQK_
H2BK34ac	_K(ac)ESYSIYVYK_
H2BK46ac	_VLK(ac)QVHPDTGISSK_
H3K9ac	_K(ac)STGGK(ac)APR_
H3K14ac	_K(ac)STGGK(ac)APR_
H3K18ac	_K(ac)QLATK(ac)AAR_
H3K23ac	_K(ac)QLATK(ac)AAR_
H3K27ac	_K(ac)SAPATGGVKKPHR_
H3K79ac	_EIAQDFK(ac)TDLR_
H3K122ac	_VTIMPK(ac)DIQLAR_
H4K12ac	_GLGK(ac)GGAK(ac)R_
H4K16ac	_GLGK(ac)GGAK(ac)R_
H4K20ac	_K(ac)VLRDNIQGITKPAIR_
H4K79ac	_K(ac)TVTAMDVVYALKR_

the identified lysine acetylated peptides in core histones in romidepsin and TSA treated cells are listed in Table IV.

Finally, we quantified dynamic change in global protein abundance of the chromatin modifying proteins in HDACI-induced bladder cancer cells. Unexpectedly, we found that the protein levels of HDAC1, HDAC2 and HDAC3 in the deacety-lation complexes of Mi-2/NuRD, CoREST, NcoR, SMRT and Sin3 were all downregulated in both romidepsin and TSA treated cells. As seen in Table V, treatment with romidepsin and TSA induced 2- and 1.7-fold downregulation for HDAC1, 3.2- and 2-fold downregulation for HDAC2, and 5.5- and 2.2-fold downregulation for HDAC3, respectively. The levels

Table V. The differentially expressed chromatin modifying proteins in response to histone deacetylase inhibitor treatment in bladder cancer 5637 cells.

Accession no.	Protein name	Symbol	Complex	Protein function	Protein level (ppm)		
					Untreated	Romidepsin	TSA
2498443	Histone deacetylase 1	HDAC1	Mi-2/NuRD; CoREST; Sin 3	Lysine deacetylase	374.75	189.09	224.75
68068066	Histone deacetylase 2	HDAC2	Mi-2/NuRD; CoREST; Sin 3	Lysine deacetylase	421.20	131.42	213.11
3334210	Histone deacetylase 3	HDAC3	Mi-2/NuRD; NcoR/SMRT	Lysine deacetylase	87.32	15.77	40.49
74717977	Histone deacetylase complex subunit SAP130	SP130	Sin 3	Repressor	17.83	6.44	8.26
68053233	Sin3 histone deacetylase corepressor complex component SDS3	SDS3	Sin 3	Corepressor	37.98	0	26.42
3334209	Histone acetyltransferase type B catalytic subunit	HAT1	KATs	Lysine acetyltransferase	52.02	48.34	103.42
215274095	Histone acetyltransferase KAT6A	KAT6A	KATs	Lysine acetyltransferase	1.55	3.37	2.16

TSA, trichostatin A.

of Sin3 histone deacetylase corepressor complex component SDS3, a regulatory protein that augments histone deacetylase activity of HDAC1, were also reduced in response to exposure to romidepsin or TSA (Table V). Additionally, romidepsin and TSA decreased the levels of histone deacetylase complex subunit SAP130 by 2.8- and 2.2-fold, respectively, in the 5637 cells. In contrast, the levels of the lysine acetyltransferase KAT6A and histone acetyltransferase type B catalytic subunit, the latter acetylates histone H4 at H4K5ac and H4K12ac, were both elevated following the HDACI induction (Table V). These data suggest that romidepsin and TSA induced global acetylation in core histones and non-histone proteins are mediated partly through the elevated levels of HATs and reduced levels of HDACs in 5637 bladder cancer cells.

Discussion

Although HDACIs such as romidepsin and vorinostat (SAHA) have been approved for the treatment of CTCL, there is no currently approved HDACI for any solid tumor indication; therefore, we explored the potential for the development of HDACI as a novel therapeutic for bladder urothelial carcinoma. In the present study, we have demonstrated that romidepsin, SAHA and TSA suppressed cell growth and caused cell death in 5637 bladder cancer cells *in vitro*. Furthermore, our quantitative proteomic studies showed that 2472 proteins were 2-fold upregulated and 2049 proteins were 2-fold downregulated in this model in response to romidepsin and TSA exposure, among them 1082 ≥2-fold upregulated proteins and 1140 ≥2-fold downregulated proteins were common to both romidepsin and TSA treatment, as compared to the untreated controls (P<0.05). The subsequent bioinformatic analysis revealed that

those differentially expressed proteins were mainly involved in biological and metabolic functions and cell death associated pathways. HDACI exposure also enhanced global acetylation levels in both histone and non-histone proteins. Twenty-three lysine acetylation marks were detected on core histones in HDACI-treated bladder cancer cells including two newly identified histone Kac sites (H2AK118ac and H2BK34ac). These data suggest that HDACI-induced alterations in protein expression is mediated, at least in part, through histone modification, leading to changes in biological and metabolic functions and cell death in bladder cancer cells. By establishing the link between histone modification and whole proteome in response to HDACI treatment, this study may deepen our understanding of HDACI-mediated therapeutics in bladder cancer.

A major goal of the chemotherapy of human malignancies is the inhibition of cell proliferation, and drug-induced cancer cell growth arrest is mediated partly by blocking cell cycle progression (23). The eukaryotic cell cycle is regulated via the sequential activation and inactivation of cyclin-dependent kinases (CDKs) that drive cell cycle progression through the phosphorylation and dephosphorylation of regulatory proteins (24-26). The activities of CDKs are positively regulated by cyclins and negatively regulated by CDK inhibitors (CKIs). Thus, the cell cycle is regulated by cyclins, CDKs and CKIs. Changes in the expression of specific CDKs or their regulatory proteins such as cyclins and CKIs can lead to uncontrolled cell proliferation and eventually to carcinogenesis (25,27). Whereas, downregulating the levels of cyclins or upregulating CKIs lead to blockade of cell cycle progression.

In this study, we showed that romidepsin and TSA downregulated the protein expression of cyclins B1/B2 and upregulated the expression of anaphase promoting complex-1

(APC1) and 14-3-3 proteins in 5637 cells. Cyclin B binds to and activates CDK1. The complex of cyclin B and CDK1 is responsible for the control of G2/M checkpoint, while APC1 acts by mediating ubiquitination and degradation of cyclin B and subsequent inactivation of CDK1. On the other hand, CDK1 activity is suppressed via phosphorylation of Thr-14 and Tyr-15 by the Wee-1 protein kinase (28) and is activated by CDC25 protein phosphatases, which function to remove the inhibitory phosphates from CDK1 (29). 14-3-3 proteins are involved in the regulation of G2/M checkpoint by 14-3-3-mediated CDC25 inactivation and Wee-1 activation. Romidepsin and TSA caused reduced levels of cyclin B and elevated levels of APC1 and 14-3-3 proteins in 5637 cells, suggesting that romidepsin and TSA suppress bladder cancer cell proliferation through cell cycle blockade at the G2/M phase, and that this occurs via the HDACI downregulation of cyclin B and upregulation of APC1 and 14-3-3 proteins, leading to cell cycle arrest and cell growth suppression in bladder cancer cells.

The other goal of cancer chemotherapy is to commit tumor cells to death or apoptosis following exposure to anticancer agents. Apoptosis is a highly regulated cellular process between cell proliferation and cell death and drug-induced cell death is mediated, at least in part, by apoptotic cell death (30).

In the present study, we found that the levels of caspase-3 were significantly increased in 5637 cells following treatment with romidepsin or TSA. In addition, both romidepsin and TSA enhanced Bax and Bak expression and triggered phosphorylation of Bcl-2 at Ser-70. It is known that the expression of pro-apoptotic proteins is mediated through p53-dependent and -independent pathways. In this study, we showed that the levels of p53 protein as well as other p53-pathway proteins, such as DNA-dependent protein kinase (PRKDC), were not elevated in response to HDACI exposure (Fig. 3A), and we confirmed by DNA sequencing that p53 gene is mutated in this cell line (data not shown), suggesting that the increased expression of apoptosis-associated proteins is not under direct control by p53 in 5637 bladder carcinoma cells. Additionally, it has been shown that phosphorylation of Bcl-2 is induced by several drugs in a panel of cancer cell lines derived from leukemia, lymphoma, and breast and prostate cancer (31-35). Phosphorylation of Bcl-2 is cell cycle-dependent, occurs at G2/M (34) and results in concomitant apoptosis (34,36). Interestingly, treatment with HDACIs was found to induce Bcl-2 Ser-70 phosphorylation at the G2/M phase of the cell cycle, with concomitant apoptosis in bladder cancer cells. This is consistent with the literature reporting that Bcl-2 phosphorylation at Ser-70 and loss of anti-apoptotic function in response to antitumor drugs and subsequent elimination of tumor cells via apoptosis (35). These results suggest that a similar mechanism (Bcl-2 phosphorylation at G2/M) may be involved with induction of apoptosis by HDACIs in this model system. Taken together, these data strongly support the involvement of Bcl-2 family proteins in HDACI-induced apoptosis, possibly acting through a p53-independent, mitochondria-dependent intrinsic apoptotic pathway in human bladder cancer 5637 cells.

A wide range of DNA damage can be inflicted, both from extracellular agents including some antitumor drugs and via endogenous mechanisms (37). Genotoxic cancer therapeutics such as cisplatin and mitomycin C bind to DNA, forming adducts that in turn can be repaired by the DNA repair machinery or lead to permanent DNA damage. Anticancer agent-induced DNA damage leads to transient arrest in the G1, S, G2 and M phases of the cell cycle, allowing cells to have sufficient time to repair damaged DNA before resuming cell cycle progression. However, severe DNA injury that is too extensive for intracellular repair mechanisms will lead to activation of intrinsic apoptosis pathway and cell death. Although DNA damage also affects normal cells, tumor cells are often more vulnerable because of defects in DNA repair pathways or critical cell cycle checkpoints.

Five main mechanisms are involved in DNA repair: i) base excision repair, which corrects non-bulky damage; ii) nucleotide excision repair, which corrects lesions that disrupt the double helical structure of DNA; iii) mismatch repair, which corrects replication errors; iv) double-strand break repair, which corrects double-strand breaks through two different pathways, homologous recombination and non-homologous end-joining; and v) direct repair, which corrects methylated or alkylated bases (38). Although the DNA lesions induced directly by HDACIs or indirectly via endogenous mechanisms such as the generation of free radicals, as well as the relevant DNA repair mechanisms responsible for the removal of those lesions in 5637 cells are still not known, our proteomic analysis revealed that the levels of multiple DNA repair proteins in multiple repair mechanisms were decreased in HDACI-treated bladder cancer cells. For example, the protein expression of XRCC1 and PARP1/2 in base excision repair, XPC and ERCC3 in nucleotide excision repair, RAD50 and MRE11A in homologous recombination, and XRCC5 and XRCC6 in non-homologous end-joining were all reduced after romidepsin and TSA treatment. The downregulation of DNA repair protein expression by HDACIs significantly impairs cellular DNA repair activity and DNA damage response, which in turn results in inhibition of transcription, replication, and chromosome segregation leading to blockade of cell cycle progression or apoptosis in bladder carcinoma cells.

Studies suggest oxidative stress as a mechanism to the primary modes of action of antitumor agents. Oxidative stress is a redox (reduction-oxidation) disequilibrium state, in which the generation of ROS overwhelms the antioxidant defense mechanisms (39). ROS such as superoxide and hydroxyl radicals are highly toxic, as a result of their actions as oxidizing agents and can have damaging effects on cell physiology. Under conditions that can cause oxidative stress, cells are exposed to excessive ROS that can oxidize membrane fatty acids, initiating lipid peroxidation, oxidize proteins (40) and cause DNA damage (41). At high level, excessive ROS may cause severe damage to cells, including necrosis and apoptosis (42).

Redox state in the cell is regulated by redox proteins. In this study, we found that romidepsin and TSA downregulated the expression of glutathione reductase (GSHR) and thioredoxin reductase 2 (TRXR2) and upregulated the expression of xanthine dehydrogenase/oxidase (XDH), which lead to ROS formation in 5637 cells. These findings suggest that oxidative stress is involved in the antitumor effects of HDACIs in bladder cancer and that exposure to HDACIs may alter the antioxidant defense system and redox mechanisms in cells. This notion is supported by the reports from other researchers demonstrating that HDACIs induce cell death through ROS production (43).
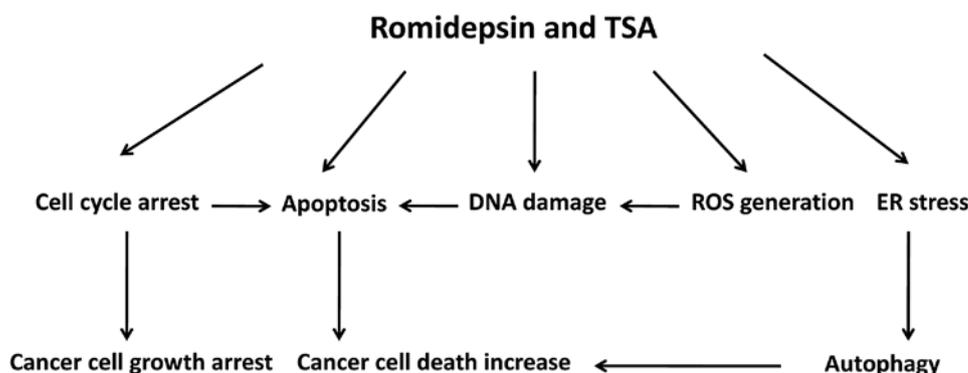
Romidepsin and TSA

Figure 5. Potential pathways involved in the induction of cell cycle arrest and apoptotic cell death by romidepsin and trichostatin A (TSA) in bladder cancer. Proteomic analysis identified 97 differentially expressed proteins that were commonly regulated by both romidepsin and TSA when compared to untreated control cells (Table II). These proteins are involved in cell cycle progression, apoptosis process, DNA damage repair, oxidative stress and autophagy regulation. See the text for details. ER, endoplasmic reticulum; ROS, reactive oxygen species.

Although the mechanism for the link between HDACI-induced oxidative stress and cell death is not well understood, several lines of evidence suggest that HDACIs induce cell death via ROS generation by the following mechanisms: i) excess of ROS may facilitate the detachment of cytochrome *c* from the mitochondrial membrane and increases the mobilized pool of cytochrome *c*, which is a prerequisite for its release into the cytoplasm through the pores created by pro-apoptotic Bcl-2 family members such as Bax and Bak; ii) ROS may also directly damage mitochondrial membrane and induce membrane potential loss that favors cytochrome *c* release; iii) death receptor aggregation may also result from ROS production and induce cell death through a different pathway; iv) downregulation of anti-apoptotic molecules and/or upregulation of pro-apoptotic signals are involved in ROS-induced cell death (44); and v) HDACI-induced ROS causes oxidative DNA damage (43), as evidenced by the levels of phosphorylated histone H2AX (γ-H2AX) and ataxia telangiectasia mutated (ATM), early markers of DNA damage, significantly increase after the administration of HDACIs (45,46). Cellular oxidative DNA damage induced by endogenous ROS production via HDACI treatment can lead to bladder cancer cell death (47).

Combining our results discussed above, we propose a possible mechanism by which HDACIs cause bladder cancer cell growth arrest and cell death as shown in Fig. 5. In this model, HDACIs alter changes in the levels and activities of proteins involved in the signaling pathways of cell cycle progression, apoptotic cell death, DNA damage repair, ROS generation, endoplasmic reticulum (ER) stress (48-50) and autophagy regulation (51), which are associated with cell death. In the proposed pathways depicted here (Fig. 5), romidepsin and TSA induce cell cycle arrest and apoptotic cancer cell death; cell cycle blockade not only causes cancer cell growth arrest, but prolonged cell cycle arrest also triggers cell suicide, usually in the form of apoptosis. In addition, the HDACIs increase DNA damage directly or indirectly through ROS production, which in turn promotes apoptosis. On the other hand, romidepsin and TSA mediate cancer cell death via inducing ER stress and autophagy. Because HDACIs target cell survival and cell death through multiple closely related but distinct mechanisms, they may act collaboratively or synergistically to promote apoptotic death of bladder cancer

cells through these signaling pathways and their downstream molecular events.

Finally, our data indicate that dysregulation of protein expression in HDACI-treated 5637 cells was associated with enhanced lysine acetylation in histone and non-histone proteins as well as alterations in the levels of chromatin modifying proteins, suggesting a role for epigenetic modification.

The three main epigenetic mechanisms (DNA methyltion, histone modifications and RNA-mediated gene silencing) have been studied primarily in the context of gene expression (52,53). The second epigenetic mechanism encompasses various histone modifications, including acetylation, glycosylation, methylation, phosphorylation and ubiquitination of specific residues in the N-terminal tails of histones (54). Histone modifications are post-translational alterations of histone proteins that interact with DNA to form a complex known as chromatin (54). Besides regulating several cellular processes including gene transcription, proliferation, and autophagy, histone modifications also affect many other chromatin-based processes such as DNA repair, replication and recombination (54).

The best-studied histone modification is lysine acetylation. The acetylation of histone modulates transcription by altering the accessibility of DNA to proteins, such as transcriptional regulators (transcriptional activators and repressors), and binding of regulatory proteins (transcription factors or repressors) to the promoter sequence of a gene resulting in activation or blocking of transcription. Furthermore, the activity of non-histone proteins, such as transcription factors and repressors, can also be modulated by post-translational protein modifications (e.g., acetylation, phosphorylation or glycosylation), and these modifications could change protein conformation and lead to changes in activity.

As the variety of gene expression profiles is determined by distinct sets of transcriptional regulators (transcription factors or repressors) that control and determine which genes are switched on or off, HDACIs may upregulate or downregulate gene expression via altering the activity of transcription factors or repressors by post-translational modifications (PTMs) in our bladder tumor cells. Additionally, since the majority of cellular functions are carried out by proteins, HDACIs may modulate biological changes not only through alterations at

the protein level but also by PTMs in bladder carcinoma cells. However, the role of the two newly identified histone markers (H2AK118ac and H2BK34ac) in the antitumor activity of HDACIs in bladder cancer, as well as the precise mechanism for how HDACIs upregulate or downregulate specific gene and protein expression through histone modifications and PTMs will require further investigation.

In summary, we have profiled the antitumor activity of HDACIs in association with enhanced lysine acetylation in histone and non-histone proteins as well as altered levels of chromatin modifying proteins in bladder cancer cells. Proteomic data analysis further revealed dysregulation of protein expression involved in multiple biological functions and cell death associated pathways in romidepsin and TSA treated 5637 cells. These results suggest that the antitumor effect of HDACIs in bladder carcinoma is mediated through modulation of these pathways by histone modifications and PTMs, leading to cancer cell growth arrest and cell death. Our findings may be helpful for developing HDCAIs in combination with other therapeutics targeted at modulating relevant cell death pathways or at inhibiting cell proliferation in tumors. Further studies are needed to investigate the anticancer activity of HDACIs in bladder cancer via the modulation of signaling pathways (e.g., PI3K-PTEN-mTOR pathway) (55) or the inhibition of regulatory enzymes in histone modifications and PTMs (56) influencing cell survival and death.

Acknowledgements

References

1. Siegel RL, Miller KD and Jemal A: Cancer statistics, 2016. CA Cancer J Clin 66: 7-30, 2016.
2. Kaufman DS, Shipley WU and Feldman AS: Bladder cancer. Lancet 374: 239-249, 2009.
3. Weintraub MD, Li QQ and Agarwal PK: Advances in intravesical therapy for the treatment of non-muscle invasive bladder cancer (Review). Mol Clin Oncol 2: 656-660, 2014.
4. Stenzl A, Cowan NC, De Santis M, Kuczyk MA, Merseburger AS, Ribal MJ, Sherif A and Witjes JA; European Association of Urology (EAU): Treatment of muscle-invasive and metastatic bladder cancer: Update of the EAU guidelines. Eur Urol 59: 1009-1018, 2011.
5. Marks P, Rifkind RA, Richon VM, Breslow R, Miller T and Kelly WK: Histone deacetylases and cancer: Causes and therapies. Nat Rev Cancer 1: 194-202, 2001.
6. Xu WS, Parmigiani RB and Marks PA: Histone deacetylase inhibitors: Molecular mechanisms of action. Oncogene 26: 5541-5552, 2007.
7. Marks PA and Xu WS: Histone deacetylase inhibitors: Potential in cancer therapy. J Cell Biochem 107: 600-608, 2009.
8. Schrump DS: Cytotoxicity mediated by histone deacetylase inhibitors in cancer cells: Mechanisms and potential clinical implications. Clin Cancer Res 15: 3947-3957, 2009.
9. Nakagawa M, Oda Y, Eguchi T, Aishima S, Yao T, Hosoi F, Basaki Y, Ono M, Kuwano M, Tanaka M, *et al*: Expression profile of class I histone deacetylases in human cancer tissues. Oncol Rep 18: 769-774, 2007.
10. Zhang Z, Yamashita H, Toyama T, Sugiura H, Ando Y, Mita K, Hamaguchi M, Hara Y, Kobayashi S and Iwase H: Quantitation of HDAC1 mRNA expression in invasive carcinoma of the breast. Breast Cancer Res Treat 94: 11-16, 2005.
11. Marquard L, Poulsen CB, Gjerdrum LM, de Nully Brown P, Christensen IJ, Jensen PB, Sehested M, Johansen P and Ralfkiaer E: Histone deacetylase 1, 2, 6 and acetylated histone H4 in B- and T-cell lymphomas. Histopathology 54: 688-698, 2009.
12. Witt O, Deubzer HE, Milde T and Oehme I: HDAC family: What are the cancer relevant targets? Cancer Lett 277: 8-21, 2009.
13. Ozawa A, Tanji N, Kikugawa T, Sasaki T, Yanagihara Y, Miura N and Yokoyama M: Inhibition of bladder tumour growth by histone deacetylase inhibitor. BJU Int 105: 1181-1186, 2010.
14. Bolden JE, Peart MJ and Johnstone RW: Anticancer activities of histone deacetylase inhibitors. Nat Rev Drug Discov 5: 769-784, 2006.
15. Minucci S and Pelicci PG: Histone deacetylase inhibitors and the promise of epigenetic (and more) treatments for cancer. Nat Rev Cancer 6: 38-51, 2006.
16. Yoshida M, Kijima M, Akita M and Beppu T: Potent and specific inhibition of mammalian histone deacetylase both in vivo and in vitro by trichostatin A. J Biol Chem 265: 17174-17179, 1990.
17. Tan J, Cang S, Ma Y, Petrillo RL and Liu D: Novel histone deacetylase inhibitors in clinical trials as anti-cancer agents. J Hematol Oncol 3: 5, 2010.
18. McGraw AL: Romidepsin for the treatment of T-cell lymphomas. Am J Health Syst Pharm 70: 1115-1122, 2013.
19. Li QQ, Wang G, Liang H, Li JM, Huang F, Agarwal PK, Zhong Y and Reed E: β-Elemene promotes cisplatin-induced cell death in human bladder cancer and other carcinomas. Anticancer Res 33: 1421-1428, 2013.
20. Florens L, Carozza MJ, Swanson SK, Fournier M, Coleman MK, Workman JL and Washburn MP: Analyzing chromatin remodeling complexes using shotgun proteomics and normalized spectral abundance factors. Methods 40: 303-311, 2006.
21. Paoletti AC, Parmely TJ, Tomomori-Sato C, Sato S, Zhu D, Conaway RC, Conaway JW, Florens L and Washburn MP: Quantitative proteomic analysis of distinct mammalian Mediator complexes using normalized spectral abundance factors. Proc Natl Acad Sci USA 103: 18928-18933, 2006.
22. Ou JN, Torrisani J, Unterberger A, Provençal N, Shikimi K, Karimi M, Ekström TJ and Szyf M: Histone deacetylase inhibitor Trichostatin A induces global and gene-specific DNA demethylation in human cancer cell lines. Biochem Pharmacol 73: 1297-1307, 2007.
23. Swanton C: Cell-cycle targeted therapies. Lancet Oncol 5: 27-36, 2004.
24. Morgan DO: Principles of CDK regulation. Nature 374: 131-134, 1995.
25. Sherr CJ: Cancer cell cycles. Science 274: 1672-1677, 1996.
26. Dynlacht BD: Regulation of transcription by proteins that control the cell cycle. Nature 389: 149-152, 1997.
27. Wesierska-Gadek J, Gueorguieva M and Horky M: Dual action of cyclin-dependent kinase inhibitors: Induction of cell cycle arrest and apoptosis. A comparison of the effects exerted by roscovitine and cisplatin. Pol J Pharmacol 55: 895-902, 2003.
28. Parker LL, Sylvestre PJ, Byrnes MJ III, Liu F and Piwnica-Worms H: Identification of a 95-kDa WEE1-like tyrosine kinase in HeLa cells. Proc Natl Acad Sci USA 92: 9638-9642, 1995.
29. Mitra J and Enders GH: Cyclin A/Cdk2 complexes regulate activation of Cdk1 and Cdc25 phosphatases in human cells. Oncogene 23: 3361-3367, 2004.
30. Fisher DE: Apoptosis in cancer therapy: Crossing the threshold. Cell 78: 539-542, 1994.
31. Haldar S, Chintapalli J and Croce CM: Taxol induces bcl-2 phosphorylation and death of prostate cancer cells. Cancer Res 56: 1253-1255, 1996.
32. Blagosklonny MV, Schulte T, Nguyen P, Trepel J and Neckers LM: Taxol-induced apoptosis and phosphorylation of Bcl-2 protein involves c-Raf-1 and represents a novel c-Raf-1 signal transduction pathway. Cancer Res 56: 1851-1854, 1996.
33. Blagosklonny MV, Giannakakou P, el-Deiry WS, Kingston DG, Higgs PI, Neckers L and Fojo T: Raf-1/bcl-2 phosphorylation: A step from microtubule damage to cell death. Cancer Res 57: 130-135, 1997.
34. Haldar S, Basu A and Croce CM: Bcl2 is the guardian of microtubule integrity. Cancer Res 57: 229-233, 1997.
35. Haldar S, Basu A and Croce CM: Serine-70 is one of the critical sites for drug-induced Bcl2 phosphorylation in cancer cells. Cancer Res 58: 1609-1615, 1998.
36. Chang BS, Minn AJ, Muchmore SW, Fesik SW and Thompson CB: Identification of a novel regulatory domain in Bcl-X(L) and Bcl-2. EMBO J 16: 968-977, 1997.

37. Roos WP, Thomas AD and Kaina B: DNA damage and the balance between survival and death in cancer biology. Nat Rev Cancer 16: 20-33, 2016.
38. Friedberg EC, Walker GC, Siede W and Schultz RA: DNA Repair and Mutagenesis. 2nd edition. ASM Press, Washington, DC, 2006.
39. Halliwell B: Free radicals, antioxidants, and human disease: Curiosity, cause, or consequence? Lancet 344: 721-724, 1994.
40. Brot N, Weissbach L, Werth J and Weissbach H: Enzymatic reduction of protein-bound methionine sulfoxide. Proc Natl Acad Sci USA 78: 2155-2158, 1981.
41. Demple B and Linn S: 5,6-Saturated thymine lesions in DNA: Production by ultraviolet light or hydrogen peroxide. Nucleic Acids Res 10: 3781-3789, 1982.
42. Xia T, Kovochich M, Brant J, Hotze M, Sempf J, Oberley T, Sioutas C, Yeh JI, Wiesner MR and Nel AE: Comparison of the abilities of ambient and manufactured nanoparticles to induce cellular toxicity according to an oxidative stress paradigm. Nano Lett 6: 1794-1807, 2006.
43. Feng R, Oton A, Mapara MY, Anderson G, Belani C and Lentzsch S: The histone deacetylase inhibitor, PXD101, poten-tiates bortezomib-induced anti-multiple myeloma effect by induction of oxidative stress and DNA damage. Br J Haematol 139: 385-397, 2007.
44. Rosato RR, Maggio SC, Almenara JA, Payne SG, Atadja P, Spiegel S, Dent P and Grant S: The histone deacetylase inhibitor LAQ824 induces human leukemia cell death through a process involving XIAP down-regulation, oxidative injury, and the acid sphingomyelinase-dependent generation of ceramide. Mol Pharmacol 69: 216-225, 2006.
45. Feng R, Ma H, Hassig CA, Payne JE, Smith ND, Mapara MY, Hager JH and Lentzsch S: KD5170, a novel mercaptoketone-based histone deacetylase inhibitor, exerts antimyeloma effects by DNA damage and mitochondrial signaling. Mol Cancer Ther 7: 1494-1505, 2008.
46. Rosato RR, Almenara JA, Maggio SC, Coe S, Atadja P, Dent P and Grant S: Role of histone deacetylase inhibitor-induced reactive oxygen species and DNA damage in LAQ-824/fludara-bine antileukemic interactions. Mol Cancer Ther 7: 3285-3297, 2008.
47. Orrenius S, Gogvadze V and Zhivotovsky B: Mitochondrial oxidative stress: Implications for cell death. Annu Rev Pharmacol Toxicol 47: 143-183, 2007.
48. Rao R, Nalluri S, Fiskus W, Savoie A, Buckley KM, Ha K, Balusu R, Joshi A, Coothankandaswamy V, Tao J, et al: Role of CAAT/enhancer binding protein homologous protein in panobinostat-mediated potentiation of bortezomib-induced lethal endoplasmic reticulum stress in mantle cell lymphoma cells. Clin Cancer Res 16: 4742-4754, 2010.
49. Rao R, Nalluri S, Kolhe R, Yang Y, Fiskus W, Chen J, Ha K, Buckley KM, Balusu R, Coothankandaswamy V, et al: Treatment with panobinostat induces glucose-regulated protein 78 acetyla-tion and endoplasmic reticulum stress in breast cancer cells. Mol Cancer Ther 9: 942-952, 2010.
50. Kahali S, Sarcar B, Prabhu A, Seto E and Chinnaiyan P: Class I histone deacetylases localize to the endoplasmic reticulum and modulate the unfolded protein response. FASEB J 26: 2437-2445, 2012.
51. Yi C, Ma M, Ran L, Zheng J, Tong J, Zhu J, Ma C, Sun Y, Zhang S, Feng W, et al: Function and molecular mechanism of acetylation in autophagy regulation. Science 336: 474-477, 2012.
52. Hassler MR and Egger G: Epigenomics of cancer - emerging new concepts. Biochimie 94: 2219-2230, 2012.
53. Jerónimo C and Henrique R: Epigenetic biomarkers in urological tumors: A systematic review. Cancer Lett 342: 264-274, 2014.
54. Bannister AJ and Kouzarides T: Regulation of chromatin by histone modifications. Cell Res 21: 381-395, 2011.
55. Abbosh PH, McConkey DJ and Plimack ER: Targeting signaling transduction pathways in bladder cancer. Curr Oncol Rep 17: 58, 2015.
56. O'Rourke CJ, Knabben V, Bolton E, Moran D, Lynch T, Hollywood D and Perry AS: Manipulating the epigenome for the treatment of urological malignancies. Pharmacol Ther 138: 185-196, 2013.